Image-guided Cardiac Interventions Using Contemporary Mid-Field Magnetic Resonance Imaging

Adrienne E Campbell-Washburn[1]

[1]National Heart, Lung, and Blood Institute, National Institutes of Health, Bethesda, USA

Abstract

Real-time MRI-guided cardiac catheter-based procedures can leverage the improved tissue contrast and functional information provided by MRI. However, clinical adoption has been hampered by a lack of safe and conspicuous devices for the MRI environment. Contemporary mid-field MRI, which pairs modern imaging methods and system hardware with a lower magnetic field strength, may offer substantial advantages for these procedures. Mid field MRI reduces device heating, while real-time imaging remains high quality. Moreover, these systems may be more accessible, and enable novel lung imaging for a comprehensive cardiopulmonary assessment that includes imaging and invasive hemodynamic measurements. This article will describe the use of mid field MRI, specifically 0.55T, for MRI-guided cardiac interventions.

1. Introduction

Real-time interactive MRI has been used to guided minimally invasive catheter-based procedures [1]. Typical real-time MRI provides imaging frame rates of 4-10 frames per second, although more rapid imaging is possible with specialized sequences [2, 3]. Real-time images are displayed to an interventionist in the scanner room who is navigating a device (Figure 1A). For the purposes of procedural guidance, these real-time pulse sequences are designed to be interactive, meaning that operators can change the image orientation, image contrast, slice thickness, and image acceleration on-the-fly.

Traditionally, catheter-based procedures are guided using bi-plane X-Ray. X-Ray lacks soft tissue contrast and provides only projection imaging, but it offers excellent visualization of catheter and guidewire devices. By comparison, MRI provides exceptional soft-tissue contrast, 3D anatomy, and functional information (e.g., cardiac function by cine imaging and flow quantification).

During these procedures, catheter-based devices are navigated from a peripheral vascular access point to the heart. In patients, several MRI-guided procedures have been performed, including invasive hemodynamic catheterization, electrophysiology and RF-ablation in the right atrium and ventricle. Moreover, in animal models, MRI-guidance has been demonstrated for endomyocardial biopsy, extra-anatomic bypass, stenting, chemoablation, and ventricular tachycardia ablation [1, 4, 5].

MRI-guided diagnostic right heart catheterization is the most common clinical application of MRI-guidance. This procedure has been performed in hundreds of patients worldwide [6-10]. The goal of MRI-guided right heart catheterization is to pair invasive chamber pressure measurements with accurate MRI measurements of flow, which provides a robust measurement of pulmonary vascular resistance at rest and during physiological stress, thus offering diagnostic value to patients. MRI-guided right heart catheterization is especially valuable in paediatric patients (e.g., single ventricle, pre/post Fontan, pulmonary hypertension) since combined cardiac MRI and catheterization provides more information in a single anaesthesia session with reduced radiation exposure. Moreover, navigation in complex congenital anatomy is easier with MRI visualization, and finally, the MRI and hemodynamic information is acquired at the same preload/afterload, generating more meaningful data.

Despite the value for patients, the clinical adoption of MRI-guided catheterization has been slow. Primarily, this is because of the lack of safe and conspicuous devices (guidewires and catheters) that can be used for procedures [11]. In many patients, right heart catheterization can be performed with only polymer catheter devices. Catheters are visualized by gadolinium or air in the balloon tip.

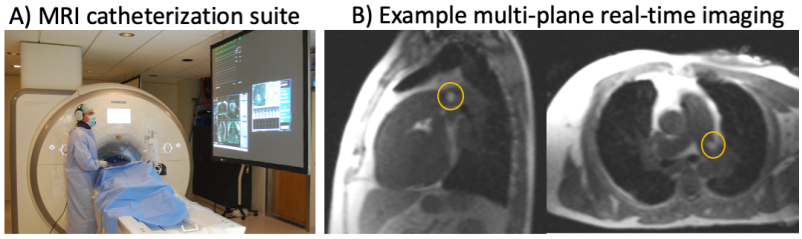

Figure 1. A) Photo of MRI-guided catheterization suite with imaging displayed for interventionist. B) Example multi-planar interactive real-time bSSFP images, with partial saturation pulse, at 0.55T. Orange circles show contrast-filled balloon at the tip of the catheter in the left pulmonary artery.

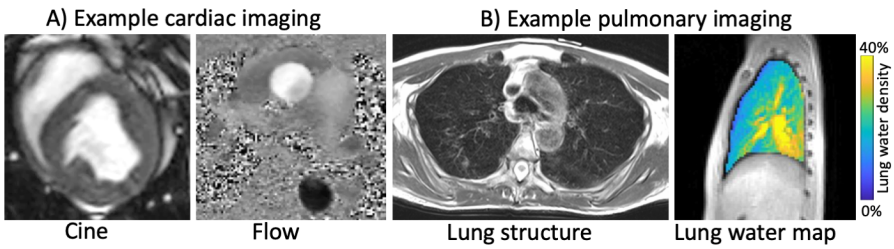

Figure 2. (A) Example cardiac imaging (cine and flow), and (B) example pulmonary imaging (structure and lung water map) from the contemporary 0.55T MRI system.

However, in patients with abnormal anatomy or physiology, a stiffer metallic guidewire is required for navigation. Furthermore, to perform more complex procedures and left-sided procedures, metallic guidewires are a requirement. These metallic guidewires are conductive and can heat during real-time MR imaging. Alternatively, polymer guidewires have been explored and are commercially available [9, 10], but are often mechanically inferior compared to metal. The inability to use off-the-shelf devices and a dearth of MRI-specific devices is a deterrent to interventionists.

We have proposed mid-field (0.55T) MRI as a solution to enable MRI-guided catheter procedures [12]. Device heating is quadratic with field strength, meaning that 0.55T MRI offers 7.5-fold less heating compared to 1.5T, and 30-fold less heating than 3T. We ramped down a 1.5T system to 0.55T to assess the value of 0.55T MRI for MRI-guided catheterization procedures. This contemporary MRI system is equipped with modern hardware and software to maintain high quality imaging at the lower field strength. More recently, a commercial version of a contemporary 0.55T system has been made available [13]. Lower field systems are inherently lower cost, which is attractive to increase the accessibility of MRI-guided catheterization procedures. This article describes the ongoing work performing ICMR at 0.55T, as presented at Computing in Cardiology 2023.

2. Imaging technology

Mid-field MRI systems were common in the 1990s and 2000s, including at 0.5T "double donut" interventional MRI system [14]. Since then, significant improvements have been made in system hardware, including main magnetic field homogeneity, gradient performance, and receiver coil arrays, as well as software, including pulse sequence design, advanced image reconstruction, and processing methods. Therefore, revisiting 0.55T MRI with a contemporary MRI system and modern imaging methods, provides a unique opportunity.

For fast imaging, there are inherent benefits to lower field MRI. Namely, T1 is shorter enabling shorter TRs; T2 and T2* are longer, enabling longer readouts; field homogeneity is better allowing sequence flexibility; and SAR is lower enabling shorter and higher power RF pulses. Together, these physical properties permit rapid imaging, including optimally designed balanced steady-state free precession (bSSFP) sequences [15, 16].

Advanced reconstruction methods, such as constrained reconstructions, are also critical to recovering SNR at lower field. Remarkable similarity between field strengths has been demonstrated using constrained reconstructions [17, 18]. Artificial intelligence offers an opportunity to improve image quality through image reconstruction and denoising. For example, a transformer model has been used to increase SNR with a standard parallel imaging reconstruction [19], and a proprietary denoiser has been used for dark blood cardiac imaging [20].

3. Cardiac and pulmonary imaging

Accurate diagnostic cardiac imaging capabilities at 0.55T are essential for MRI-guided catheterization procedures (Figure 2A). Previous publications have demonstrated that assessment of left and right ventricular function and volumes can be accurately quantified in patients at 0.55T [17], and quantitative flow measurements have been shown to be consistent at 0.35T [21] and 0.55T [22]. Moreover, tissue viability imaging, namely scar size using late gadolinium enhancement has been validated [23]. A comprehensive cardiac MRI protocol has also been demonstrated using a commercial 0.55T system [20].

A novel application of 0.55T is pulmonary imaging [12]. The contemporary 0.55T system design offers improved B0 field homogeneity, meaning that there is less susceptibility at air-tissue interfaces. As a result, high quality imaging of the lung parenchyma is possible (Figure 2B) and is comparable to lung CT [24]. MRI also offers unique capabilities in regional assessment of lung function (e.g., ventilation and perfusion) [25-27]. Finally, methods to image pulmonary oedema have been developed to evaluate exercise-induced lung water accumulation in patients with heart failure [28, 29]. These pulmonary imaging developments are relevant to MRI-guided cardiac catheterization procedures because often patients undergoing right heart catheterization have conditions that may affect both their lungs and heart (e.g., pulmonary hypertension and heart failure).

4. MRI-guided catheterization procedures at 0.55T

Campbell-Washburn et al described MRI-guided right heart catheterization in 7 patients at 0.55T[12]. Importantly, this study used an off-the-shelf nitinol

guidewire and standard Cartesian real-time bSSFP imaging without parameter modification (Figure 1B). This was the first study of its kind to use an unmodified metallic device and standard imaging for this procedure in patients. The study also demonstrated negligible RF-induced heating (<1 °C during 2 minutes of real-time imaging) in 9 of the 16 nitinol guidewires and stainless-steel braided catheters tested. Devices that were fully-insulated and shorter are more likely safe. Özen et al tested an additional four commercial devices for hepatic artery and coronary artery intervention, and demonstrated safety at 0.55T [30]. These results demonstrate the potential use of standard off-the-shelf metallic devices for MRI-guided procedures, and to potentially enable more complex procedures.

Device visualization can be challenging at 0.55T due to the reduced susceptibility artifacts. Artifact size depends on metal alloy, with nitinol and stainless-steel 316 generating field-strength dependent artifacts and stainless-steel 304 (with higher tensile strength) saturated at field strengths <0.55T, meaning that artifact size if field-strength independent in the 0.55T to 3T range [31]. These results suggest that standard nitinol guidewires have reduced visibility at 0.55T, but that stainless-steel markers could be designed to generate consistent artifacts across field strengths. Alternatively, "active visualization" by which a device is designed as a receiver coil, can provide highly specific visualization. Yilidirm et al have designed an active guidewire with a curved-tip geometry that is safe-by-design at 0.55T and demonstrated clear visualization in vivo in a swine model [32]. Additionally, Yilidirm et al have developed a method of thin-film circuit printing to print active device circuitry onto an existing device for 0.55T [33].

Visualization of RF and chemoablation lesions is critical for MRI-guided electrophysiology and ablation procedures, and has been demonstrated at 0.55T[34]. Notably, both lesion types were visible with T1 weighted imaging, and chemoablation generated a more pronounced T1 shortening than RF ablation, which improved conspicuity. Additionally, MRI-guided invasive pressure-volume loop measurements have been demonstrated by combining invasive pressure measurements with real-time cine cardiac volume measurements [35]. This study demonstrated differences in contractility and compliance by measuring pressure-volume loops during a pre-load alteration (inferior vena cava balloon inflation) in an animal model of cardiomyopathy.

Commercial 0.55T MRI systems offer lower gradient specifications, and therefore rapid real-time imaging is more challenging. Nevertheless, MRI-guided catheterization and stent deployment have been demonstrated in swine [36]. This is encouraging to indicate that a commercially available system may be capable of the procedures described in this article with the advantages of 0.55T described herein.

5. Conclusions

Mid-field (0.55T) MRI offers unique advantages for MRI-guided interventions by virtue of reduced device heating, robust cardiac imaging, improved pulmonary imaging, and increased system accessibility. The 0.55T platform is powerful for combined cardiopulmonary assessment with both imaging and hemodynamics for diagnosis. Moreover, the ability to use off-the-shelf metallic devices, and to develop new devices more easily, offers potential for more advanced MRI-guided procedures in patients in the future.

Acknowledgments

The author thanks Robert Lederman, Toby Rogers, Kanishka Ratnayaka, Daniel Herzka, Rajiv Ramasawmy, and Felicia Seemann for their collaboration on MRI-guided catheterization at 0.55T. Siemens Healthcare assisted in the modification of the MRI system for operation at 0.55T under an existing cooperative research agreement (CRADA) between NHLBI and Siemens Healthcare. This work was funded by NHLBI DIR (Z01-HL006257, Z01-HL006213, Z01-HL006039).

References

1. Rogers T, Campbell-Washburn AE, Ramasawmy R, Yildirim DK, Bruce CG, Grant LP, et al. Interventional cardiovascular magnetic resonance: state-of-the-art. J Cardiovasc Magn Reson. 2023;25(1):48.
2. Campbell-Washburn AE, Tavallaei MA, Pop M, Grant EK, Chubb H, Rhode K, et al. Real-time MRI guidance of cardiac interventions. J Magn Reson Imaging. 2017;46(4):935-50.
3. Campbell-Washburn AE, Faranesh AZ, Lederman RJ, Hansen MS. Magnetic resonance sequences and rapid acquisition for MR-guided interventions. Magn Reson Imaging Clin N Am. 2015;23(4):669-79.
4. Ratnayaka K, Faranesh AZ, Guttman MA, Kocaturk O, Saikus CE, Lederman RJ. Interventional cardiovascular magnetic resonance: still tantalizing. J Cardiovasc Magn Reson. 2008;10:62.
5. Mukherjee RK, Chubb H, Roujol S, Razavi R, O'Neill MD. Advances in real-time MRI-guided electrophysiology. Curr Cardiovasc Imaging Rep. 2019;12(2):6.
6. Rogers T, Ratnayaka K, Khan JM, Stine A, Schenke WH, Grant LP, et al. CMR fluoroscopy right heart catheterization for cardiac output and pulmonary vascular resistance: results in 102 patients. J Cardiovasc Magn Reson. 2017;19(1):54.
7. Ratnayaka K, Kanter JP, Faranesh AZ, Grant EK, Olivieri LJ, Cross RR, et al. Radiation-free CMR diagnostic heart catheterization in children. J Cardiovasc Magn Reson. 2017;19(1):65.
8. Pushparajah K, Tzifa A, Razavi R. Cardiac MRI catheterization: a 10-year single institution experience and review. Interventional Cardiology. 2014;6(3).
9. Knight DS, Kotecha T, Martinez-Naharro A, Brown JT, Bertelli M, Fontana M, et al. Cardiovascular magnetic resonance-guided right heart catheterization in a conventional

CMR environment - predictors of procedure success and duration in pulmonary artery hypertension. J Cardiovasc Magn Reson. 2019;21(1):57.
10. Veeram Reddy SR, Arar Y, Zahr RA, Gooty V, Hernandez J, Potersnak A, et al. Invasive cardiovascular magnetic resonance (iCMR) for diagnostic right and left heart catheterization using an MR-conditional guidewire and passive visualization in congenital heart disease. J Cardiovasc Magn Reson. 2020;22(1):20.
11. Rogers T, Lederman RJ. Interventional CMR: Clinical applications and future directions. Curr Cardiol Rep. 2015;17(5):580.
12. Campbell-Washburn AE, Ramasawmy R, Restivo MC, Bhattacharya I, Basar B, Herzka DA, et al. Opportunities in interventional and diagnostic imaging by using high-performance low-field-strength MRI. Radiology. 2019:190452.
13. SiemensHealthineers. Press Release: MAGNETOM Free.Max. Available from: https://www.siemens-healthineers.com/press/releases/magnetom-free-max.html.
14. Schenck JF, Jolesz FA, Roemer PB, Cline HE, Lorensen WE, Kikinis R, et al. Superconducting open-configuration MR imaging system for image-guided therapy. Radiology. 1995;195(3):805-14.
15. Restivo MC, Ramasawmy R, Bandettini WP, Herzka DA, Campbell-Washburn AE. Efficient spiral in-out and EPI balanced steady-state free precession cine imaging using a high-performance 0.55T MRI. Magn Reson Med. 2020;84(5):2364-75.
16. Hamilton JI, Truesdell W, Galizia M, Burris N, Agarwal P, Seiberlich N. A low-rank deep image prior reconstruction for free-breathing ungated spiral functional CMR at 0.55 T and 1.5 T. MAGMA. 2023.
17. Bandettini WP, Shanbhag SM, Mancini C, McGuirt DR, Kellman P, Xue H, et al. A comparison of cine CMR imaging at 0.55 T and 1.5 T. J Cardiovasc Magn Reson. 2020;22(1):37.
18. Simonetti OP, Ahmad R. Low-field cardiac magnetic resonance imaging: A compelling case for cardiac magnetic resonance's future. Circ Cardiovasc Imaging. 2017;10(6).
19. Xue H, Javed A, Ramasawmy R, Rehman A, Kellman P, Campbell-Washburn AE. CNNT denoising for cine imaging at 0.55T with higher acceleration rates. Proceedings from the 25th Annual SCMR Scientific Sessions2023.
20. Varghese J, Jin N, Giese D, Chen C, Liu Y, Pan Y, et al. Building a comprehensive cardiovascular magnetic resonance exam on a commercial 0.55 T system: A pictorial essay on potential applications. Frontiers in Cardiovascular Medicine. 2023;10.
21. Varghese J, Crabtree C, Craft J, Liu Y, Jin N, Ahmad R, et al. Cine and flow imaging at 0.35 T and Comparison to 3T. SCMR. 2019:P238.
22. Shanbhag SM, Ramasawmy R, Bandettini WP, Mancini CM, McGuirt DR, Henry JL, et al. Comparison of phase-contrast flow imaging at 0.55T and 1.5T. Proceedings of the ISMRM Annual Meeting2020. p. 2256.
23. Bandettini WP, Shanbhag SM, Mancini C, Henry JL, Lowery M, Chen MY, et al. Evaluation of myocardial infarction by cardiovascular magnetic resonance at 0.55-T compared to 1.5-T. JACC Cardiovasc Imaging. 2021;14(9):1866-8.
24. Campbell-Washburn AE, Malayeri AA, Jones EC, Moss J, Fennelly KP, Olivier KN, et al. T2-weighted lung imaging using a 0.55-T MRI system. Radiology: Cardiothoracic Imaging. 2021;3(3):e200611.
25. Bhattacharya I, Ramasawmy R, Javed A, Lowery M, Henry J, Mancini C, et al. Assessment of lung structure and regional function using 0.55 T MRI in patients with lymphangioleiomyomatosis. Invest Radiol. 2022;57(3):178-86.
26. Bhattacharya I, Ramasawmy R, Javed A, Chen MY, Benkert T, Majeed W, et al. Oxygen-enhanced functional lung imaging using a contemporary 0.55 T MRI system. NMR Biomed. 2021:e4562.
27. Levy S, Heiss R, Grimm R, Grodzki D, Hadler D, Voskrebenzev A, et al. Free-breathing low-field MRI of the lungs detects functional alterations associated with persistent symptoms after COVID-19 infection. Invest Radiol. 2022;57(11):742-51.
28. Seemann F, Javed A, Chae R, Ramasawmy R, O'Brien K, Baute S, et al. Imaging gravity-induced lung water redistribution with automated inline processing at 0.55 T cardiovascular magnetic resonance. J Cardiovasc Magn Reson. 2022;24(1):35.
29. Seemann F, Javed A, Khan JM, Bruce CG, Chae R, Yildirim DK, et al. Dynamic lung water MRI during exercise stress. Magn Reson Med. 2023;90(4):1396-413.
30. Ozen AC, Russe MF, Lottner T, Reiss S, Littin S, Zaitsev M, et al. RF-induced heating of interventional devices at 23.66 MHz. MAGMA. 2023.
31. Basar B, Sonmez M, Yildirim DK, Paul R, Herzka DA, Kocaturk O, et al. Susceptibility artifacts from metallic markers and cardiac catheterization devices on a high-performance 0.55 T MRI system. Magn Reson Imaging. 2021;77:14-20.
32. Yildirim DK, Uzun D, Bruce CG, Khan JM, Rogers T, Schenke WH, et al. An interventional MRI guidewire combining profile and tip conspicuity for catheterization at 0.55T. Magn Reson Med. 2023;89(2):845-58.
33. Yildirim DK, Bruce C, Uzun D, Rogers T, O'Brien K, Ramasawmy R, et al. A 20-gauge active needle design with thin-film printed circuitry for interventional MRI at 0.55T. Magn Reson Med. 2021;86(3):1786-801.
34. Kolandaivelu A, Bruce CG, Ramasawmy R, Yildirim DK, O'Brien KJ, Schenke WH, et al. Native contrast visualization and tissue characterization of myocardial radiofrequency ablation and acetic acid chemoablation lesions at 0.55 T. J Cardiovasc Magn Reson. 2021;23(1):50.
35. Seemann F, Bruce CG, Khan JM, Ramasawmy R, Potersnak AG, Herzka DA, et al. Dynamic pressure-volume loop analysis by simultaneous real-time cardiovascular magnetic resonance and left heart catheterization. J Cardiovasc Magn Reson. 2023;25(1):1.
36. Armstrong A, Krishnamurthy R, Swinning J, LIU Y, Joseph M, Jin N, et al. Feasibility of MRI-Guided cardiac catheterization, angioplasty, and stenting in a 0.55T scanner with limited gradient performance. Proceedings from the 25th Annual SCMR Scientific Sessions2023.

Address for correspondence:

Adrienne E. Campbell-Washburn, PhD
National Heart, Lung, and Blood Institute
National Institutes of Health
10 Center Dr.
Building 10, Rm B1D219
Bethesda, Maryland
USA 20892
adrienne.campbell@nih.gov